Microdroplet Mass Spectrometry

DOI: 10.1002/anie.201310795

On-Chip Spyhole Mass Spectrometry for Droplet-Based Microfluidics**

*Natalia Gasilova, Qiuliyang Yu, Liang Qiao, and Hubert H. Girault**

Abstract: *For efficient coupling of droplet-based microfluidics with mass spectrometry (MS), a spyhole drilled on the top of a microchip is used to sample the passing droplets by electrostatic-spray ionization (ESTASI) MS. The technique involves placing an electrode below the chip under the spyhole and applying high-voltage pulses. Electrospray occurs directly from the spyhole, and the droplet content is analyzed by MS without a dilution or oil removal step. To demonstrate the versatility of this technique, we have successfully monitored a droplet-based tryptic digestion, as well as a biphasic reaction between β-lactoglobulin in water and α-tocopheryl acetate in 1,2-dichloroethane, where the protein extracts the antioxidant from the oil phase and becomes reduced.*

Microfluidic devices for water-in-oil microdroplet handling have found a wide range of applications in various scientific fields.[1] Organic,[1,2] inorganic,[3] and biological synthesis,[4,5] kinetic studies,[2,6] and immunoassays[7] are enhanced in droplets owing to the low sample consumption, fast reagent mixing, short reaction time, and precise process control.[1,2] Protein crystallization,[8] biological screening,[9,10] microseparation techniques,[11,12] and different single-cell experiments[13] also benefit from the advantages of droplet-based microfluidic systems.

The variety of droplet applications requires the integration of different detection methods into the microfluidic devices, for example, fluorescence and electrochemical detection.[1,14] Mass spectrometry (MS) is a powerful alternative to couple with microfluidics owing to its sensitivity and analyte mass spectrum as a clear readout.[15] Electrospray ionization (ESI) MS has been successfully employed for droplets analysis, but its coupling to these systems still remains challenging.[16] The presence of oil as carrier fluid compromises the ionization efficiency and ESI plume stability.[17] To overcome this limitation, the droplets need to be isolated from the oil, for example, by their transfer to MS coupled aqueous flow using electrical pulses,[16] hydrophilic surface coating,[18] or adding a sheath-flow.[19] However, these techniques lead to dilution and sample zone spreading. Optimized microchip design can partially decrease the dilution factor and improve the sensitivity.[20] Another possibility is to create water–air droplets[21] or switch to the analysis in off-line mode using ESI[17,22] or matrix-assisted laser desorption ionization (MALDI)[23] MS. The first approach suffers from droplets merging owing to air compression, while the two others possess the drawbacks of off-line analysis. The direct transfer of the water–oil plugs to MS is also possible with perfluorodekalin (PFD) as oil phase[24] or with surfactant addition to the droplet system.[25]

Herein, we present a novel approach for coupling droplet-based microfluidics with MS using the recently introduced electrostatic-spray ionization (ESTASI)[26] method to monitor single-phase and biphasic reactions. In comparison with the traditional ESI, one of the main advantages of this technique is the performance of dilution-free droplet ionization without the additional oil removal step. It was realized on-line in a simple manner without an assisting sheath-flow or surfactant addition and provided high detection sensitivity. The polyimide (PI) microchip fabricated by laser ablation[26] was designed with a spyhole through which the water droplets were ionized when passing through the microchannel underneath (Figure 1).

The ionization of the water-in-oil droplets generated with an average volume of 3 nL (RSD = 7%, $n = 20$) and 0.1 Hz frequency was realized by the contactless application of high-voltage (HV) square pulses with an electrode placed under the microchip and aligned with the spyhole and MS inlet (see the Supporting Information Movie for illustration). Absence of a direct contact with the sample prevented any electrochemical reactions. Optimized microchip parameters, such as a 50 μm spyhole diameter and 100 μm for microchannel depth and width, provided reproducible ESTASI without any solution leakage from the spyhole. The RSD of total cation current (TCC) and single cation current (SCC) intensities for the analysis of the droplets containing 3 μM peptide angiotensin I were 16% and 15% ($n = 20$), respectively, with a stable signal frequency of 0.1 Hz (RSD = 5%, $n = 20$). The optimization of the microchip parameters and of the droplet generation is described in details in the Supporting Information, Sections SI-1 and SI-2, respectively.

During the MS analysis of droplets through the spyhole, the oil continued flowing to the microchip outlet to be adsorbed by a swab stick, thus avoiding any contamination to the ion source. As a complete synchronization of droplet generation frequency with HV pulses and MS scans remained challenging, the HV frequency of 10 Hz was used for a droplet generation frequency of about 0.1 Hz to insure the ionization

[*] N. Gasilova,[+] Q. Yu,[+] Dr. L. Qiao, Prof. Dr. H. H. Girault
Laboratoire d'Electrochimie Physique et Analytique
Ecole Polytechnique Fédérale de Lausanne
Station 6, 1015 Lausanne (Switzerland)
E-mail: hubert.girault@epfl.ch
Homepage: http://lepa.epfl.ch

[+] These authors contributed equally to this work.

[**] This work was supported by the Swiss National Science Foundation grant "Front-end functional microchips for mass spectrometry (200020-144512)".

Supporting information for this article, including specifications of the chemicals and the equipment used, is available on the WWW under http://dx.doi.org/10.1002/anie.201310795.

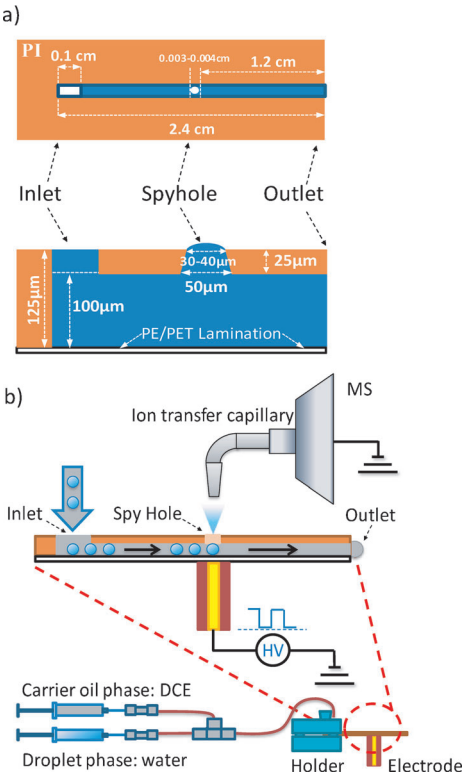

Figure 1. Microchip and setup designs. a) Top and longitudinal views of the PI microchip with a spyhole. b) The setup used for the droplets coupling with ESTASI MS. Droplets generated in capillaries were transferred to the microchip by a homemade plastic holder. An electrode was placed under the spyhole to apply HV pulses (0 to 8 kV) for ESTASI of water droplets passing by, while the oil continued to flow towards the microchip outlet.

of all produced water droplets (see the Supporting Information, Section SI-2 for more details). To decrease the negative effect of the oil presence in the system, 1,2-dichloroethane (DCE) was chosen as the carrier oil phase owing to its low viscosity and low interference with sample electrospray in contrast with fluorinated oils.[17,20] The high amplitude of the HV pulses also provided efficient analyte ionization and sensitive MS detection. As a consequence, only a slight TCC decrease (Figure 2) and increase of the limit of detection (LOD) value were observed owing to the DCE presence, while other tested oils provided either an unstable ESTASI signal for droplets, like PFD, or no signal at all (see the Supporting Information, Section SI-2 for more details). It is worth mentioning that as a pulsed ionization process, ESTASI also provides pulsed MS signals for the continuous sample flow. For the model peptide angiotensin I (1296.5 Da), the LOD was 10 nM for droplets instead of 5 nM for a continuous sample flow, and 70 nM instead of 30 nM for the protein cytochrome C (12384 Da) (Figure 2b,c; Supporting Information, Figure SI-1.4). In this case, sample droplets contained 50% methanol, 49% deionized water, and 1% acetic acid (ESI solution). However, the presence of organic solvent and acidic pH in the water phase was not necessary, as for conventional ESI. The ESTASI mechanism allowed satisfactory electrospray formation directly from pure water or basic pH solutions by the application of HV pulses, eliminating the necessity of assisting sheath flow. For basic pH droplets, the MS spectra were mainly composed of ion peaks with lower charge states due to the lower concentration of protons (Figure 2d).

To check the sample carry-over in the spyhole microchip a linear concentration gradient was created in the droplets using 5 µM acetyllysine (AcLys) solution (from 100 to 0%) and 5 µM dipeptide TyrTyr solution (from 0 to 100%) within 5 min. 5 µM of dipeptide LysVal was presented in both solutions as an internal standard to perform the relative quantification of ESTASI MS results. As presented in Figure 2e,f, the overall carry-over was 6% resulting from the sample adsorption inside the system as no leakage from the spyhole was observed during the experiment (see the Supporting Information, Section SI-3 for more details).

The present microfluidic set-up was tested first on a model single-phase reaction like in-droplets tryptic digestion of the protein cytochrome C and the hormone peptide ACTH (1–24) (2933.5 Da). ESTASI MS was successfully performed directly from the droplets with the basic digestion solution of 5 µg mL^{-1} trypsin in 25 mM NH_4HCO_3, pH 8.5, showing that the enzymatic digestion is much faster in the droplet-based system than in the bulk solution. More details are presented in the Supporting Information, Section SI-4.

The droplet-based system was further used for study of a biphasic reaction, namely the interaction between β-lactoglobulin (LGB, mixture of A, 18363 Da and B, 18276 Da isoforms) and α-tocopheryl acetate (TA, 472 Da). LGB is known as a lipocalin which binds in its cavity α-tocopherol, the most biologically active form of vitamin E, protecting it from decomposition and increasing its solubility in water.[27] In the present work, TA was chosen, as it is a more stable compound against oxidation owing to the presence of an acetic protective group. To follow the biphasic reaction by ESTASI MS, the water droplets with 5.4 µM LGB were formed using as the carrier oil phase DCE containing 135 µM TA. The results, presented in Figure 3, showed that during the complex formation, LBG oxidized TA despite the protective group presence. Such a redox reaction with LGB was not previously described, even for the more active reducing molecule of α-tocopherol.[27,28]

At the beginning, the formation of LGB-TA complex increased TA solubility in the water phase and its ionization efficiency (Figure 3a.1). In the absence of LGB in the water droplets, no MS signal from TA was recorded (Figure 3b.1), confirming the low solubility of TA in water and its large partition in DCE. The intact LGB-TA complex was not observed owing to the ESTASI process, which disrupted noncovalent interaction during the ionization. With the increase of the reaction time (defined as the time needed for freshly formed droplets to pass from the T-junction to the spyhole inside the microchip) the LGB charge distribution started to change, indicating the modification of the protein conformation. After 9.4 min of reaction, only peaks corresponding to LGB ions with 10 and 11 charges were observed together with TA and its oxidized form (Figure 3a.3). Longer reaction times resulted in partial LGB aggregation, significant decrease of its MS signal, and increase of the oxidized TA

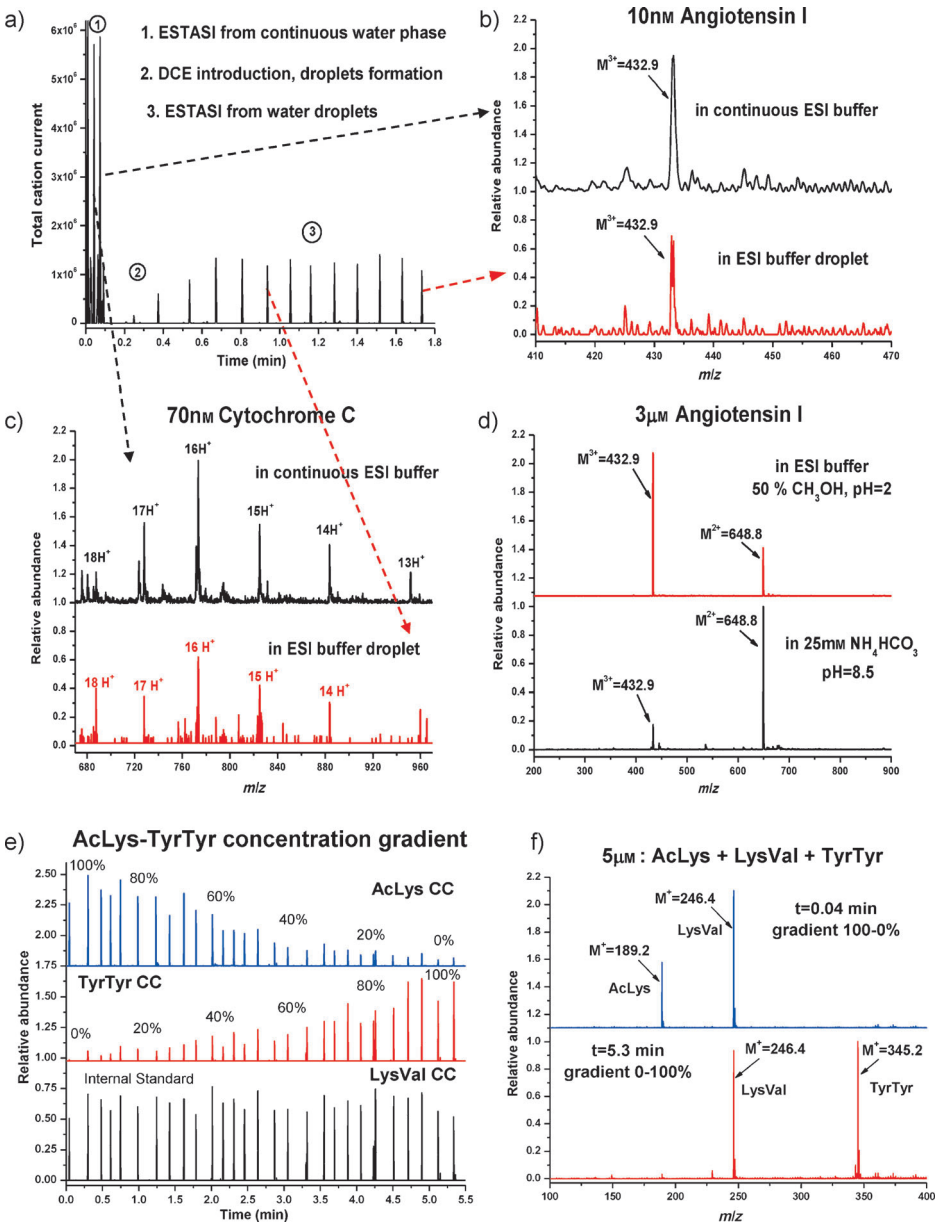

Figure 2. ESTASI MS analysis of the water-in-DCE droplets. a) TCC intensity changing with droplets formation. TCC from continuous sample flow (1) disappeared when a DCE flow was introduced (2) and reappeared with lower intensity when the formation of droplets with 0.1 Hz frequency was stabilized (3). b), c) ESTASI MS spectra collected from continuous sample flow (1) and from droplets (3) for 10 nM angiotensin I and 70 nM cytochrome C, respectively. d) ESTASI MS spectra of 3 μM angiotensin I obtained from droplets with a standard acidic ESI solution containing methanol, and with basic pH aqueous buffer. e) SCC chromatograms for AcLys-TyrTyr concentration gradient experiment with LysVal as internal standard. f) ESTASI MS spectra corresponding to 0.04 min (100:0%) and 5.3 min (0:100%) of concentration gradient.

signal (Figure 3a.4; Supporting Information, Figure SI-5.1). It could be concluded from these results that TA not only binds with LGB, but also reduces its disulfide bridges leading to protein conformational changes and a new charge distribution in the MS spectra. To confirm this redox reaction, LGB reduction with dithiothreitol (DTT) was performed separately in a bulk solution and analyzed by ESTASI-MS. As presented in Figure 3b.3, LGB reduced by DTT provided a similar charge distribution as in the case of the interaction with TA. To follow the progress of the LGB-TA redox reaction, the time dependence for the ratio between MS peak intensities of TA and oxidized TA, as well as for the ratio between LGB MS peak intensities for charge states $z = 10$ (predominant for reduced LGB) and $z = 13$ (predominant for native LGB) is shown in the Supporting Information, Figure SI-5.b,c.

Based on the obtained MS data, it was assumed that the TA oxidation product should be similar to the one of α-tocopherol, that is, α-tocopherolhydroquinone,[29] taking into account the non-radical pathway of the oxidation.[30] To define the structure of oxidized TA, the interaction between LGB in the water phase and TA in DCE was performed in a tube as a shake flask reaction. After 30 min of reaction, the water phase was analyzed by ESTASI MS, giving similar spectra as in-droplet reaction (Figure 3b.4). The collected water phase was also submitted to the conventional ESI MS for the tandem MS analysis of oxidized TA. The fragmentation results obtained (Supporting Information, Figure SI-6.b,c) confirmed the quinone structure of the TA oxidation product (Figure 3a). The acetic protective group allowed TA oxidation, which is probably due to its ability to stabilize the benzylic cation intermediate previously observed for non-radical TA nitration.[31]

To further support the occurrence of a redox reaction between LGB and TA, benzoquinone (BQ)[32] was used for the tagging of free cysteine residues formed after reduction of the LGB disulfide bridges by TA. On the obtained ESTASI and deconvoluted MS spectra (Figure 3c,d), clear mass shifts of 108 Da and 216 Da were observed owing to the one and two BQ tags in the structure of both LGB isoforms A and B. One BQ tag corresponds to the free cysteine present in native LGB.[33] The second tag formation is a result of disulfide bridge reduction by TA (for more details, see the Supporting Information, Section SI-7).

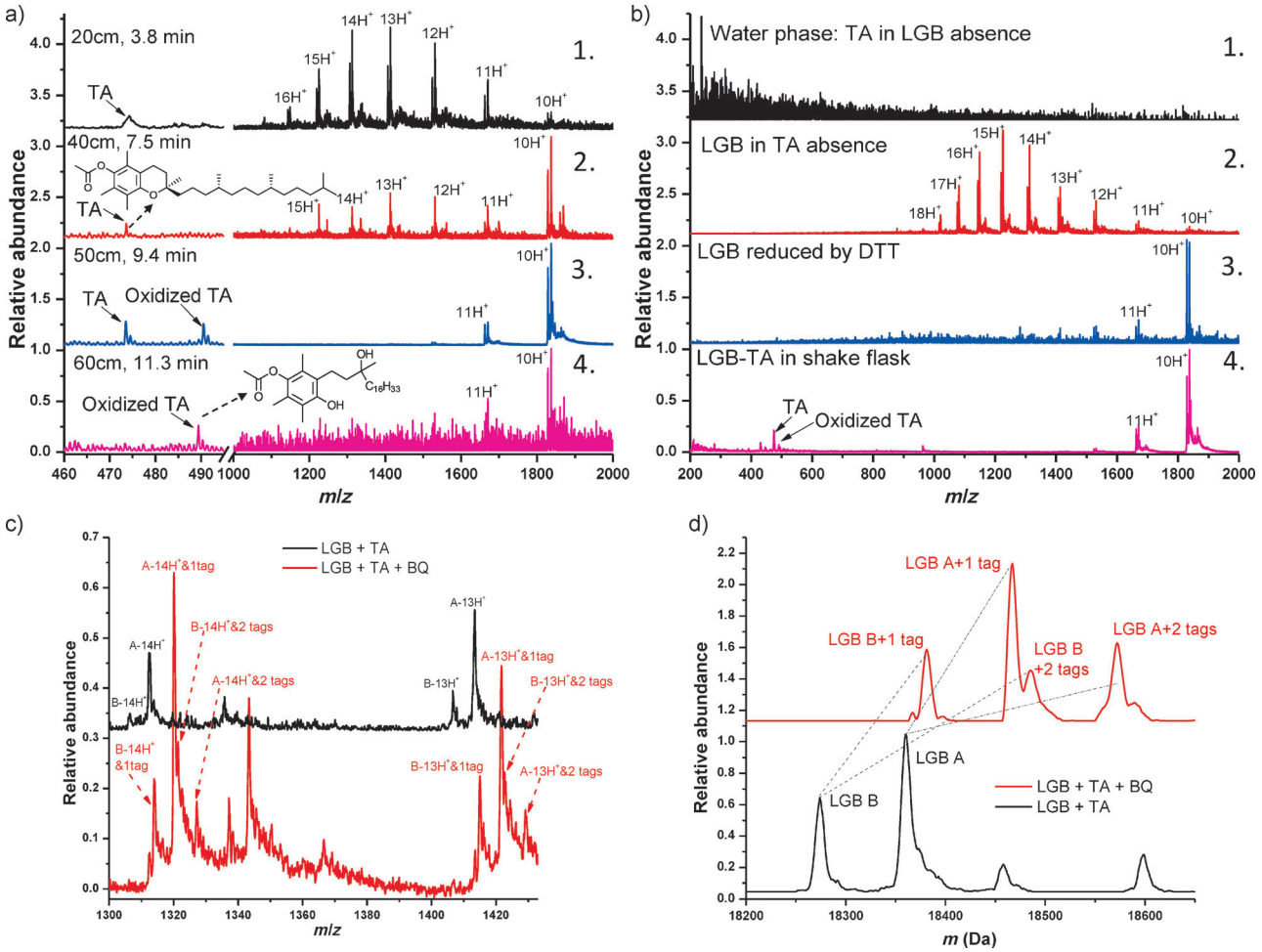

Figure 3. ESTASI MS spectra of LGB-TA biphasic reaction in droplets: 5.4 μM LGB (A + B) in the water phase and 135 μM TA in DCE. Double peak observed for each LGB charge state corresponds to the two isoforms (A + B). a) MS spectra from the droplets at various reaction times. During the reaction, LGB changed its charge distribution on MS spectra from normal (1) to the reduced molecule (3), while TA was oxidized (4). b) Control MS experiments. (1) Absence of TA MS signal without LGB in the water phase. (2) LGB normal charge distribution in the absence of TA in DCE. (3) Reduced LGB charge distribution after reaction with DTT. (4) Results of LGB and TA interaction in a shake flask reaction. c) Tagging free cysteine residues by 2.5 mM BQ in the LGB (A and B isoforms) reduced by TA. Magnified ESTASI MS spectra (charge states $z = 14$ and $z = 13$) of TA reduced LGB (black) and TA reduced LGB tagged with BQ (red). d) Deconvoluted spectra of TA reduced LGB (black) and TA reduced LGB tagged with BQ (red). A(B)-nH$^+$: n protonated A (B) isoform of LGB; A(B)-nH$^+$ & 1 (2) tag(s): n protonated A (B) isoform of LGB with one (two) BQ tag(s).

In summary, we have demonstrated that the spyhole ESTASI MS is a very powerful method to monitor on-line the performance of the droplet-based on-chip microreactors without interfering with their function. It allows dilution-free droplets ionization without an oil removal step and insures sensitive MS detection by the contactless HV application. Due to the ESTASI mechanism, droplets containing only pure water or a basic pH solution can also be efficiently ionized without any sheath-flow of organic solvent and acidic pH.

A variety of single-phase reactions in droplets can be performed and analyzed by ESTASI MS, as it was demonstrated for peptide and protein tryptic digestion. The realization of biphasic reactions, and especially those of biological relevance, is also a promising prospect. The characterization of LGB-TA binding was successfully performed, revealing new information about this interaction. More complex biphasic reactions can be studied in vitro, such as lipid oxidation and other processes that take place in living cells across the membranes.

Received: December 12, 2013
Published online: March 18, 2014

Keywords: biphasic reactions · electrostatic spray · mass spectrometry · microdroplets · microreactors

[1] A. B. Theberge et al., *Angew. Chem.* **2010**, *122*, 5982 – 6005; *Angew. Chem. Int. Ed.* **2010**, *49*, 5846 – 5868.
[2] H. Song, D. L. Chen, R. F. Ismagilov, *Angew. Chem.* **2006**, *118*, 7494 – 7516; *Angew. Chem. Int. Ed.* **2006**, *45*, 7336 – 7356.
[3] A. Abou-Hassan, O. Sandre, V. Cabuil, *Angew. Chem.* **2010**, *122*, 6408 – 6428; *Angew. Chem. Int. Ed.* **2010**, *49*, 6268 – 6286.

[4] S. Gulati, V. Rouilly, X. Niu, J. Chappell, R. I. Kitney, J. B. Edel, P. S. Freemont, A. J. deMello, *J. R. Soc. Interface* **2009**, *6 Suppl 4*, S493 – 506.
[5] B. Kintses, L. D. van Vliet, S. R. A. Devenish, F. Hollfelder, *Curr. Opin. Chem. Biol.* **2010**, *14*, 548 – 555.
[6] M. Srisa-Art, E. C. Dyson, A. J. deMello, J. B. Edel, *Anal. Chem.* **2008**, *80*, 7063 – 7067.
[7] A. Ali-Cherif, S. Begolo, S. Descroix, J.-L. Viovy, L. Malaquin, *Angew. Chem.* **2012**, *124*, 10923 – 10927; *Angew. Chem. Int. Ed.* **2012**, *51*, 10765 – 10769.
[8] B. Zheng, J. D. Tice, L. S. Roach, R. F. Ismagilov, *Angew. Chem.* **2004**, *116*, 2562 – 2565; *Angew. Chem. Int. Ed.* **2004**, *43*, 2508 – 2511.
[9] H. N. Joensson, M. L. Samuels, E. R. Brouzes, M. Medkova, M. Uhlén, D. R. Link, H. Andersson-Svahn, *Angew. Chem.* **2009**, *121*, 2556 – 2559; *Angew. Chem. Int. Ed.* **2009**, *48*, 2518 – 2521.
[10] S. Cho, D.-K. Kang, S. Sim, F. Geier, J.-Y. Kim, X. Niu, J. B. Edel, S.-I. Chang, R. C. R. Wootton, K. S. Elvira, A. J. deMello, *Anal. Chem.* **2013**, *85*, 8866 – 8872.
[11] Z. Xiao, M. Niu, B. Zhang, *J. Sep. Sci.* **2012**, *35*, 1284 – 1293.
[12] J. S. Edgar, G. Milne, Y. Zhao, C. P. Pabbati, D. S. W. Lim, D. T. Chiu, *Angew. Chem.* **2009**, *121*, 2757 – 2760; *Angew. Chem. Int. Ed.* **2009**, *48*, 2719 – 2722.
[13] H. N. Joensson, H. Andersson-Svahn, *Angew. Chem.* **2012**, *124*, 12342 – 12359; *Angew. Chem. Int. Ed.* **2012**, *51*, 12176 – 12192.
[14] Y. Zhu, Q. Fang, *Anal. Chim. Acta* **2013**, *787*, 24 – 35.
[15] P. Hoffmann, U. Häusig, P. Schulze, D. Belder, *Angew. Chem.* **2007**, *119*, 5000 – 5003; *Angew. Chem. Int. Ed.* **2007**, *46*, 4913 – 4916.
[16] L. M. Fidalgo, G. Whyte, B. T. Ruotolo, J. L. P. Benesch, F. Stengel, C. Abell, C. V Robinson, W. T. S. Huck, *Angew. Chem.* **2009**, *121*, 3719 – 3722; *Angew. Chem. Int. Ed.* **2009**, *48*, 3665 – 3668.
[17] Q. Li, J. Pei, P. Song, R. T. Kennedy, *Anal. Chem.* **2010**, *82*, 5260 – 5267.
[18] Y. Zhu, Q. Fang, *Anal. Chem.* **2010**, *82*, 8361 – 8366.
[19] J. Ji, L. Nie, L. Qiao, Y. Li, L. Guo, B. Liu, P. Yang, H. H. Girault, *Lab Chip* **2012**, *12*, 2625 – 2629.
[20] R. T. Kelly, J. S. Page, I. Marginean, K. Tang, R. D. Smith, *Angew. Chem.* **2009**, *121*, 6964 – 6967; *Angew. Chem. Int. Ed.* **2009**, *48*, 6832 – 6835.
[21] J. Pei, Q. Li, M. S. Lee, G. A. Valaskovic, R. T. Kennedy, *Anal. Chem.* **2009**, *81*, 6558 – 6561.
[22] Y. Su, Y. Zhu, Q. Fang, *Lab Chip* **2013**, *13*, 1876 – 1882.
[23] S. K. Ku, S. R. Fagerer, P. E. Verboket, K. Eyer, K. Je, R. Zenobi, P. S. Dittrich, *Anal. Chem.* **2013**, *85*, 1285 – 1289.
[24] S. Sun, T. R. Slaney, R. T. Kennedy, *Anal. Chem.* **2012**, *84*, 5794 – 5800.
[25] C. A. Smith, X. Li, T. H. Mize, T. D. Sharpe, E. I. Graziani, C. Abell, W. T. S. Huck, *Anal. Chem.* **2013**, *85*, 3812 – 3816.
[26] L. Qiao, R. Sartor, N. Gasilova, Y. Lu, E. Tobolkina, B. Liu, H. H. Girault, *Anal. Chem.* **2012**, *84*, 7422 – 7430.
[27] L. Liang, V. Tremblay-Hébert, M. Subirade, *Food Chem.* **2011**, *126*, 821 – 826.
[28] L. Liang, M. Subirade, *Food Chem.* **2012**, *132*, 2023 – 2029.
[29] D. C. Liebler, J. A. Burr, A. J. Ham, *Methods Enzymol.* **1999**, *299*, 309 – 318.
[30] A. Azzi, A. Stocker, *Prog. Lipid Res.* **2000**, *39*, 231 – 255.
[31] C. Adelwöhrer, T. Rosenau, P. Kosma, *Tetrahedron* **2003**, *59*, 8177 – 8182.
[32] T. C. Rohner, J. S. Rossier, H. H. Girault, *Electrochem. Commun.* **2002**, *4*, 695 – 700.
[33] G. Kontopidis, C. Holt, L. Sawyer, *J. Dairy Sci.* **2004**, *87*, 785 – 796.

